

## Supplementary Materials

### Localization of light induced in ordered colloidal suspensions: powerful sensing tools

Viktor A. Ermakov<sup>1,2</sup>, W. S. Martins<sup>3</sup>, Niklaus U. Wetter<sup>4</sup>, Francisco. C. Marques<sup>2</sup>, Ernesto Jiménez-Villar<sup>2,4,5\*</sup>

<sup>1</sup>*Departamento de Física, Universidade Federal de São Carlos, São Carlos, SP 13565-905, Brazil*

<sup>2</sup>*Departamento de Física Aplicada, Universidade Estadual de Campinas, Campinas SP 13083-859, Brazil*

<sup>3</sup>*Programa de Pós-Graduação em Engenharia Física, Unidade Acadêmica do Cabo de Santo Agostinho, Universidade Federal Rural de Pernambuco, Cabo de Santo Agostinho, PE 54518-430, Brazil*

<sup>4</sup>*Instituto de pesquisas Energéticas e Nucleares, CNEN/IPEN, São Paulo, SP 05508-000, Brazil*

<sup>5</sup>*Departamento de Física, Universidade Federal da Paraíba, João Pessoa PB 58051-970, Brazil*

\*Corresponding author: [Ernesto.jimenez@uv.es](mailto:Ernesto.jimenez@uv.es)

#### Materials and Methods:

Ethanol alcohol HPLC with spectroscopic grade purity and the ammonia P.A. were supplied by MERCK, tetra-ethyl-ortho-silicate (TEOS) was supplied by Sigma-Aldrich. The titanium dioxide (TiO<sub>2</sub>) with a rutile crystal structure and 4 g cm<sup>-3</sup> density was acquired from DuPont Inc. (R900). The TiO<sub>2</sub> grains have an average particle diameter of 410nm with a polydispersity of 25%. The TiO<sub>2</sub> nanoparticles (NPs) were coated with a silica shell of ~40 nm thickness via the Stöber method. In the first stage, 5 g of TiO<sub>2</sub> NPs were dispersed in 500 ml of ethanol (HPLC). This suspension was placed in an ultrasound bath for 20 minutes to disperse the particles and 6.67 mL of ammonia and 10 mL of TEOS were added. The TEOS and commercial ammonia (NH<sub>4</sub>OH 28%-30%) were added alternately in 100 portions of 100 µl and 220 µl, respectively. The synthesized TiO<sub>2</sub>@Silica NPs suspension was rota-evaporated, dried in an oven at 70 °C for 2 h. From the initial mass of TiO<sub>2</sub> NPs (5 g), a final mass of 7.75 g was obtained for the as-synthesized TiO<sub>2</sub>@Silica NPs, which represents a mass increase of 1.55 times. The powder of TiO<sub>2</sub>@Silica NPs was re-dispersed in ethanol and water at different [NPs] ([TiO<sub>2</sub>@silica]) from [7 x10<sup>10</sup> NPs ml<sup>-1</sup>] to [410 x10<sup>10</sup> NPs ml<sup>-1</sup>], which correspond to filling fractions (*FF*) of TiO<sub>2</sub> (rutile) from 0.26% to 12.1% (0.26%, 0.54%, 1.06%, 2.56%, 4.8%, 8.79% and 12.1%), respectively. [TiO<sub>2</sub>@Silica] in the suspensions were calculated as follows:

First, the mass of one TiO<sub>2</sub> NP is estimated from the mean volume of TiO<sub>2</sub> NPs (mean diameter 410 nm) and rutile density (4 g cm<sup>-3</sup>), this is, (mean TiO<sub>2</sub> NP volume x4 g cm<sup>-3</sup>). Second, the number of

the TiO<sub>2</sub>@Silica NPs is determined by the ratio of total TiO<sub>2</sub> NPs mass over TiO<sub>2</sub> NP mass. Filling fraction is defined as the volume fraction (%) occupied by the rutile TiO<sub>2</sub> NPs in the total volume of the suspension (TiO<sub>2</sub> volume x100%/suspension volume). TiO<sub>2</sub> volume and suspension volume are determined as: TiO<sub>2</sub> mass/4 g cm<sup>-3</sup> and TiO<sub>2</sub> mass/4 g cm<sup>-3</sup> plus liquid volume (ethanol or water), respectively. Suspensions of TiO<sub>2</sub> NPs without silica shell were also prepared in ethanol with approximately the same TiO<sub>2</sub> (rutile) *FF*. Additionally, two pellets with *FF* of 33% and 68% were prepared, compacting the TiO<sub>2</sub>@Silica and TiO<sub>2</sub> powders, respectively.

### Raman experiments

A Micro-Raman XploRA Horiba with a CW 532 nm laser as an excitation source was used for collecting the Raman scattering signal. For the experimental setup see Figure 1a. Samples, S, composed of TiO<sub>2</sub>@Silica NPs in ethanol or water solution, or TiO<sub>2</sub> NPs in ethanol, were suspended in different concentrations and irradiated with a CW frequency doubled Nd<sup>3+</sup>:YAG laser (532 nm). A quartz sample holder (MS) supporting 80μl of solution is covered with a BK7 cover glass (CG) of 170μm thickness. An oil-immersion Olympus 60x objective (Ob) with the biggest numerical aperture  $NA=1.41$  was used to irradiate the samples and collect the Raman signal, which allows a collection depth into the samples of 1.2 μm. For correcting the enhancement of the Raman signal by the pumping depth (depth of focus) we have taken into account the scattering lengths  $l_s$  for each sample. We considered that the mean pumping intensity ( $I_{PM}$ ) at 1.2 μm depth into the sample depends on  $l_s$  as follow:

$$I_{PM} = \frac{\int_0^{C_d} I_p(z) dz}{C_d} = \frac{I_0}{C_d} \int_0^{C_d} e^{-\frac{z}{l_s}} dz = -\frac{I_0 l_s}{C_d} \left( e^{-\frac{C_d}{l_s}} - 1 \right),$$

, where  $C_d$ ,  $I_p(z)$  and  $I_0$  are the collection depth of our

optical system (1.2 μm), the ballistic pumping intensity at  $z$  depth and the incident pumping intensity at  $z=0$ , respectively. Clearly, when  $l_s \gg C_d = 1.2 \mu\text{m}$ ,  $I_{PM} \approx I_0$ . The term  $(I_0/C_d)$  is the same for all samples. Therefore, in order to correct the enhancement factor of the Raman signal, the signal was

divided by  $-l_s \left( e^{-\frac{c_d}{l_s}} - 1 \right)$  for each sample ( $FF$ ). For  $\text{TiO}_2@\text{Silica}$  suspensions in water and ethanol,  $l_s$  values, determined experimentally, are plotted as a function of  $FF$  in figure S1b.

The enhancement of the Raman signal, reported in this study, is low compared to the surface-enhanced Raman scattering (SERS) supported by localized surface plasmon resonance in metallic structures. It is well known that SERS is limited to a reduced volume, only very close to the metallic NPs surface. However, the present phenomenon of enhancement of light-matter coupling, revealed in our samples, is observed in the whole pumped volume of the sample. The typical enhancement of electric field at the surface of a resonantly excited isolated NP (metallic) is estimated to be 30-fold. So, if we consider a 10-fold mean electric field enhancement in the 5 nm thick surrounding volume, a mean enhancement of the Raman signal by SERS of  $10^4$ -fold is expected in this surrounding volume. If this enhancement volume (5 nm thick surrounding volume) represents a volume fraction of 0.25%, the mean enhancement of the Raman signal in the whole volume of the sample would be 25-fold, which is similar to what was observed in our sample ( $FF=12.1\%$ ). This 0.25% volume fraction (in metallic NPs of 10 nm diameter) is equivalent to a concentration of metallic NPs of  $\sim 1.4 \times 10^{14}$  NPs/ml, which is  $>300$  times higher than that of our sample with  $FF=12.1\%$  ( $420 \times 10^{10}$  NPs/ml). The latter means that for a more efficient sensing process, the molecules to be detected must be very close to the metallic NPs surface. However, in our system, the enhanced light-matter coupling happens throughout the whole pumped volume.

### **Measurement of the ballistic transmission**

Figure S1a shows a schematic diagram of the experimental setup for the measurement of the ballistic transmission. The laser beam (second harmonic of a  $Q$ -switched Nd:YAG Continuum Minilite II,  $\lambda=532$  nm, 1  $\mu\text{J}$  (1mJ attenuated  $10^3$  times by neutral density filters), with a pulse width of  $\sim 4$  ns, and a repetition rate of 10 Hz) was passed through a positive lens  $L_1$  (200 mm focal length), in order to obtain the focus with its waist near the pinhole  $\text{PH}_1$  (600 $\mu\text{m}$  diameter). The cell consisted of two

optical flats F (fused silica, 5 mm thickness) that, together, formed a wedge. Thus, the slab thickness depends on the laser beam's incidence point on the cell. The laser spot size on the cell was  $\sim 0.5$  mm. Another pinhole, PH<sub>2</sub> (1200  $\mu$ m diameter), was positioned 80 mm away from PH<sub>1</sub>, in order to reduce the diffuse light. Yet another lens, L<sub>2</sub> (50 mm focal length), allowed for focalization onto the optical fiber facet (200  $\mu$ m core size). The multimode optical fiber was coupled to a spectrometer HR4000 UV-VIS (Ocean Optics) of 0.36 nm spectral resolution full-width at half-maximum (FWHM). In order to average out laser intensity fluctuations, the transmitted intensity was acquired by integration during 20s (200 laser shots). For this photon transport experiment, the laser fluence (Nd:YAG, 532 nm) on the samples was held constant (1  $\mu$ J). Several optical neutral filters were introduced in front of the optical fiber, providing a broad dynamic range of detection. In order to reduce the stray light, the fused silica plates (50 mm diameter) that formed the wedged cuvette, were glued with opaque silicone glue.

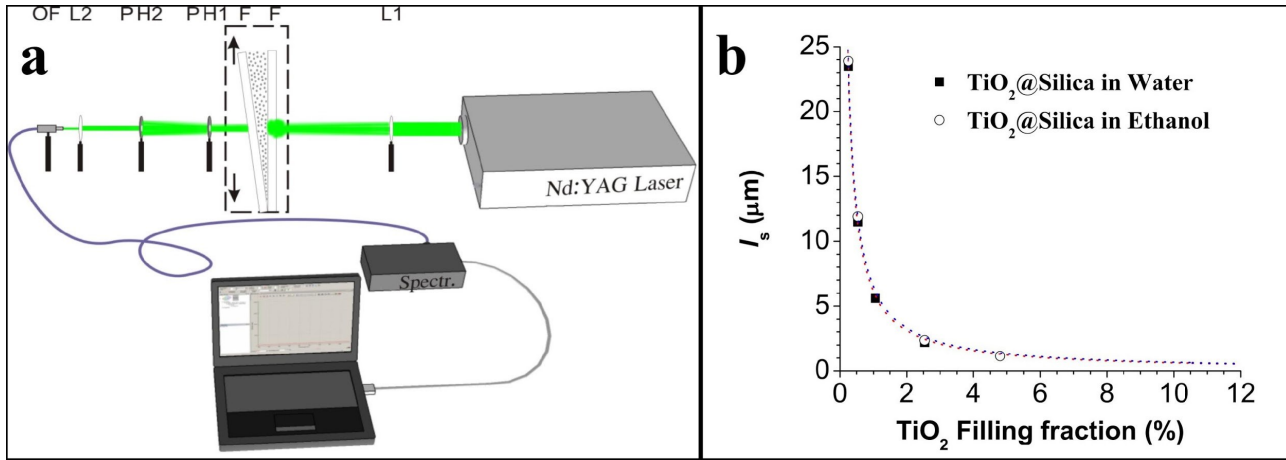


**Figure S1. Ballistic experiment.** *a)* Schematic diagrams of the experimental setup for determination of transmitted ballistic intensity as a function of slab thickness. L<sub>1</sub> and L<sub>2</sub>, are lenses; F+F, is the cell consisting of two optical flats mounted on a translation stage; PH<sub>1</sub> and PH<sub>2</sub>, are pinholes; OF, is the optical fiber to collect the light into the spectrometer. *b)* Evolution of  $I_s$  as a function of FF for the TiO<sub>2</sub>@Silica suspensions in water (closed square) and in ethanol (open circles). The blue and red dotted lines represent the fitting with the inverse functions  $FF^{-1}$  for suspensions in ethanol and water, respectively.

For TiO<sub>2</sub>@Silica NPs suspensions in water with TiO<sub>2</sub> (rutile) filling fraction (FF) of: 2.56%, 1.06%, 0.54% & 0.26%, the transmitted ballistic intensity  $I_p$  was measured as a function of the slab

thickness. The scattering mean free paths,  $l_s$ , were determined from the first experimental point of the coherent transmission curves.<sup>1</sup> For  $FF$  values of 12.1%, 8.9%, and 4.8%, the  $l_s$  values could not be determined because the intensity decayed extremely quickly. For TiO<sub>2</sub>@Silica NPs suspension in ethanol with  $FF$  of 4.8%, 2.56%, 1.06% and 0.54%, the  $l_s$  values were determined in our previous work.<sup>1</sup>  $l_s$  values extracted from the ballistic transmission decayed inversely proportional with  $FF$  (figure S1b). Taking into account this behavior,  $l_s$  values were extrapolated (pointed lines) for  $FF$  of 12.1%, 8.9% (in ethanol) and 12.1%, 8.9% & 4.8% (in water). For TiO<sub>2</sub>@Silica NPs suspensions in water, the  $l_s$  values were around 5-8% lower than those in ethanol, which agrees satisfactory with the calculus by Mie theory. Note that the refractive index of water (1.33) is slightly lower than that of ethanol (1.36). For pure TiO<sub>2</sub> NPs suspensions in ethanol with  $FF$  of 2.8% and 0.18%,  $l_s$  values, also determined by the coherent transmission curves (previous work<sup>2</sup>), are 52  $\mu\text{m}$  and 15  $\mu\text{m}$ , respectively. As can be observed,  $l_s$  values decayed slower than inversely proportional to  $FF$ , which we associated to the TiO<sub>2</sub> NPs' agglomeration. The latter indicates that for  $FF$  of 12.1%, 8.9% and 4.8%,  $l_s$  values must be several times higher than the pumping depth (1.2  $\mu\text{m}$ ), therefore, the Raman signal remains unchanged after correction by the pumping depth.

### Transmittance experiment

The intensity structure of a probe beam was studied after propagating a distance of  $\sim 1.8$  mm through the samples. Figure S2 shows a schematic diagram of the experimental setup for this study. The linearly polarized probe beam (He-Ne laser) was passed through a positive lens  $L_1$  (100 mm focal length) in order to obtain a focus with its waist near the pinhole PH (100 $\mu\text{m}$  diameter). Another lens,  $L_2$  (38 mm focal length), was positioned 250 mm away from PH, in order to focus the beam on the cell, CV. The spot size on the input face of the sample is  $<50$   $\mu\text{m}$  (FWHM). Neutral density filters

---

<sup>1</sup> E. Jimenez-Villar, I. F. Da Silva, V. Mestre, P. C. De Oliveira, W. M. Faustino and G. F. De Sá, *Nanoscale*, 2016, **8**, 10938–10946

<sup>2</sup> E. Jimenez-Villar, V. Mestre, P. C. de Oliveira, G. F. de Sá, Novel core-shell (TiO<sub>2</sub>@Silica) nanoparticles for scattering medium in a random laser: higher efficiency, lower laser threshold and lower photodegradation. *Nanoscale*. **5**, 12512–7 (2013).

were used to attenuate the beam intensity (He-Ne). The cell consisted of two optical flats (fused silica, 6 mm thickness) separated by  $\sim 1.8$  mm. In order to reduce the stray light, a metallic film with an aperture of  $\sim 5$  mm diameter, through which the probe beam enters, is placed on the substrate at the silica-sample input interface. A CCD camera collected the images of the probe beam at the output face. For the  $\text{TiO}_2@\text{Silica}$  suspensions in water and ethanol with  $FF$  below ( $FF=0.26\%$ ), around ( $FF=1.06\%$ ) and above ( $FF=4.8\%$ ) the threshold of the enhancement of the Raman signal ( $FF_{\text{onset}}$ ), the intensity profile of a Gaussian probe beam was collected after propagating through the samples. In order to obtain meaningful statistics, a total of 10 images, collected for different input points and CCD integrating times, were recorded for each sample. The integrated intensity profiles  $\left[ I = \int I(x,y) dx dy = 2\pi \int I(r) dr \right]$  were determined for each measurement. The relative transmittance  $G = \frac{I_w}{I_{\text{Eth}}}$  was determined for the above three  $FF$ , where  $I_w$  and  $I_{\text{Eth}}$  are integrated transmitted intensities for the  $\text{TiO}_2@\text{Silica}$  suspensions in water and ethanol, respectively.

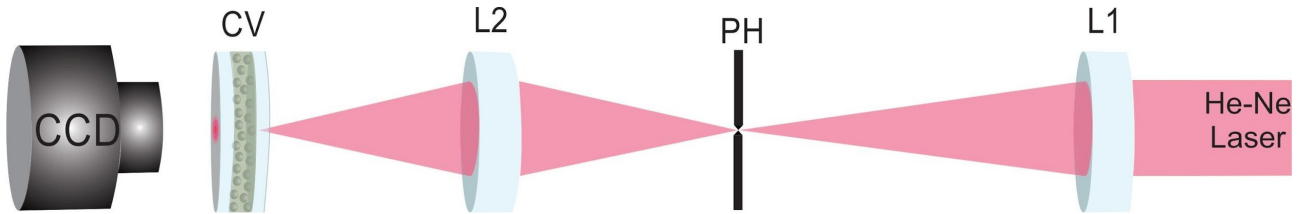


**Figure S2. Transmittance experiment.** Schematic diagram of the experimental setup for determination of the intensity profile and relative transmittance after propagating through samples.  $L_1$  and  $L_2$ , lens; PH, pinhole; CV, fused silica cuvette of  $\sim 1.8$  mm optical pathlength; CCD camera.

### Light diffraction from backscattered light

Backscattered light was collected during a short time ( $50 \mu\text{s}$ ). Diffraction pattern, coming from the first scattering event, can reveal the distribution of the scatterers' positions. For  $\text{TiO}_2@\text{Silica}$  suspensions in water and ethanol at  $FF$  below ( $FF=0.26\%$ ), around ( $FF=1.06\%$ ) and above ( $FF=4.8\%$ ) the threshold of enhancement of the Raman signal and, therefore, the onset of transition phase to localization, the light diffraction by the suspensions was studied. The experimental setup used to this end is shown in figure S3a. The linearly polarized laser beam (He-Ne) was passed through

a positive lens  $L_1$  (100 mm focal length) in order to obtain the focus with its waist near the pinhole PH (100  $\mu\text{m}$  diameter). Another lens,  $L_2$  (50 mm focal length), was positioned 200 mm away from PH in order to obtain a parallel beam on the focus with its waist ( $\sim 4.4 \mu\text{m}$  diameter) on the sample input surface. The backscattered light is collected perpendicular to the sample's surface by a CCD located at 65 mm from the sample surface. The incidence angle was  $\sim 45^\circ$  regarding to the normal, which correspond to an incidence angle inside the sample of  $\sim 26^\circ$ . In order to obtain a meaningful statistic and average the speckle pattern, a total of 400 images were recorded for each sample. The cell was composed of two fused silica optical flats (6 mm thickness).

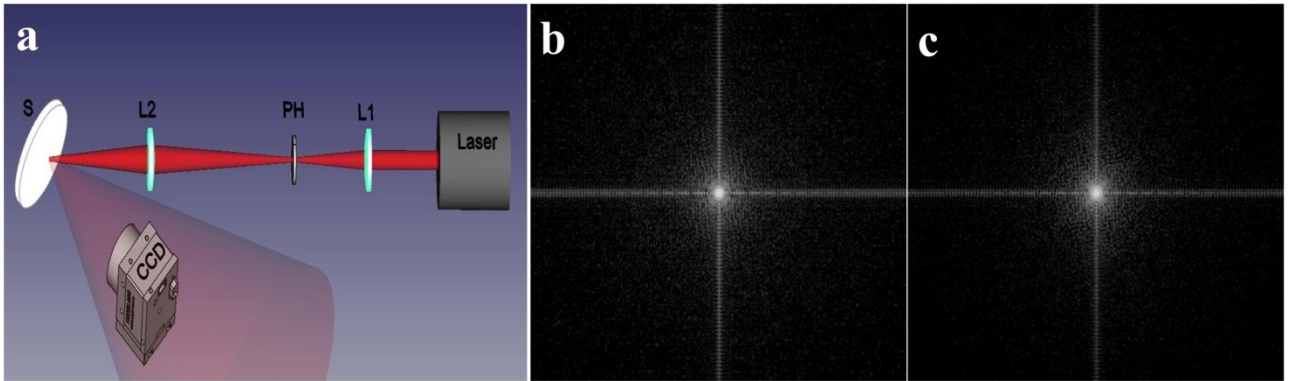


**Figure S3. Diffraction experiment.** a) *Schematic diagram of the experimental setup for collecting light diffracted by the colloidal suspension. A linearly polarized laser beam (He-Ne) was used to irradiate the samples.  $L_1$  and  $L_2$ , lens; PH, pinhole; CV, fused silica cuvette and CCD camera. b)-c) diffraction patterns for  $FF=0.26\%$  extracted from the ethanol b) and water c) suspensions.*

Figure S3b and S3c show diffraction patterns extracted from the suspensions in ethanol and water at  $FF=0.26\%$ , respectively. As can be observed, no diffraction pattern can be distinguished, which indicates a random distribution of scatterers.